Optogenetic fMRI interrogation of brain-wide central vestibular pathways

Alex T. L. Leong[a,b], Yong Gu[c], Ying-Shing Chan[d], Hairong Zheng[e], Celia M. Dong[a,b], Russell W. Chan[a,b], Xunda Wang[a,b], Yilong Liu[a,b], Li Hai Tan[f], and Ed X. Wu[a,b,d,g,1]

[a]Laboratory of Biomedical Imaging and Signal Processing, The University of Hong Kong, Pokfulam, Hong Kong SAR, China; [b]Department of Electrical and Electronic Engineering, The University of Hong Kong, Pokfulam, Hong Kong SAR, China; [c]Institute of Neuroscience, Key Laboratory of Primate Neurobiology, CAS Center for Excellence in Brain Science and Intelligence Technology, Chinese Academy of Sciences, Shanghai 200031, China; [d]School of Biomedical Sciences, Li Ka Shing Faculty of Medicine, The University of Hong Kong, Pokfulam, Hong Kong SAR, China; [e]Shenzhen Institutes of Advanced Technology, Chinese Academy of Sciences, Shenzhen 518055, China; [f]Center for Language and Brain, Shenzhen Institute of Neuroscience, Shenzhen 518057, China; and [g]State Key Laboratory of Pharmaceutical Biotechnology, The University of Hong Kong, Pokfulam, Hong Kong SAR, China

Edited by Marcus E. Raichle, Washington University in St. Louis, St. Louis, MO, and approved March 20, 2019 (received for review July 20, 2018)

Blood oxygen level-dependent functional MRI (fMRI) constitutes a powerful neuroimaging technology to map brain-wide functions in response to specific sensory or cognitive tasks. However, fMRI mapping of the vestibular system, which is pivotal for our sense of balance, poses significant challenges. Physical constraints limit a subject's ability to perform motion- and balance-related tasks inside the scanner, and current stimulation techniques within the scanner are nonspecific to delineate complex vestibular nucleus (VN) pathways. Using fMRI, we examined brain-wide neural activity patterns elicited by optogenetically stimulating excitatory neurons of a major vestibular nucleus, the ipsilateral medial VN (MVN). We demonstrated robust optogenetically evoked fMRI activations bilaterally at sensorimotor cortices and their associated thalamic nuclei (auditory, visual, somatosensory, and motor), high-order cortices (cingulate, retrosplenial, temporal association, and parietal), and hippocampal formations (dentate gyrus, entorhinal cortex, and subiculum). We then examined the modulatory effects of the vestibular system on sensory processing using auditory and visual stimulation in combination with optogenetic excitation of the MVN. We found enhanced responses to sound in the auditory cortex, thalamus, and inferior colliculus ipsilateral to the stimulated MVN. In the visual pathway, we observed enhanced responses to visual stimuli in the ipsilateral visual cortex, thalamus, and contralateral superior colliculus. Taken together, our imaging findings reveal multiple brain-wide central vestibular pathways. We demonstrate large-scale modulatory effects of the vestibular system on sensory processing.

fMRI | vestibular system | optogenetic | medial vestibular nucleus | vestibular functions

Among our sensory systems, five senses (sight, hearing, touch, smell, and taste) receive the most attention, leaving our vestibular sense as the least understood. The vestibular system senses angular and linear acceleration of the head in three dimensions via a labyrinth of sense organs in the inner ear and generates compensatory eye/body movements (i.e., vestibulo-ocular reflexes, vestibulo-spinal reflexes) that stabilize visual images on the retina and adjust posture (1–4). These interactions allow us to maintain a clear vision of our external environment, while sensing the direction and speed of our body during our actual movement. These functions strongly suggest the integration of sensory and motor systems at different regions in the vestibular system (5).

Early anatomical tracer studies in rodents (6–8), cats (9), and primates (10) showed an extensive number of axonal projections coursing into and out of the vestibular nuclei, a brainstem region that connects the inputs from vestibular sense organs in the inner ear to other regions in the central nervous system. These studies showed that the vestibular nuclei receive inputs from all sensory modalities from both their respective peripheral sense organs and thalamic regions, indicating the importance of the vestibular system in multisensory integration. One excellent example of the multisensory integration process in the vestibular system is optokinetic nystagmus, whereby visual cues are used to induce compensatory reflexive eye movements to maintain a stable gaze while moving (11, 12). These eye movements involve inputs from the vestibular labyrinth, extraocular muscle tones through the oculomotor nerve, oculomotor nucleus (OMN) in the brainstem, visual-associated thalamus and cortices, and cerebellum into the vestibular nuclei, which integrate and mediate the fast and slow phases of the nystagmus response (13–15). In addition, reciprocal projections were found between the motor cortex (M1 & M2) and vestibular nuclei (6–10), which indicates that the vestibular nuclei integrate sensory and motor information to ensure accurate motor execution and control for self-motion perception, another key multisensory integration process in the vestibular system (4). Using diffusion-based magnetic resonance imaging (MRI) tractography, studies also found the existence of these projections in humans (16). Emerging evidence indicates that the vestibular system also plays a vital role in cognition (3, 5, 17), as spatial memory deficits occur following lesions to vestibular nuclei or sense organs (18, 19). Taken together, these studies highlight the multimodal nature of vestibular processing. We need comprehensive in vivo brain-wide investigations to reveal key regions vital in processing vestibular sensory information.

Significance

The vestibular system provides a critical role to coordinate balance and movement, yet it remains an underappreciated sense. Functional MRI (fMRI) reveals much information about brain-wide sensory and cognitive processes. However, fMRI mapping of regions that actively process vestibular information remains technically challenging, as it can permit only limited movement during scanning. Here, we deploy fMRI and optogenetic stimulation of vestibular excitatory neurons to visualize numerous brain-wide central vestibular pathways and interrogate their functional roles in multisensory processing. Our study highlights multiple routes to investigate vestibular functions and their integration with other sensory systems. We reveal a method to gain critical knowledge into this critical brain system.

Author contributions: A.T.L.L. and E.X.W. designed research; A.T.L.L. and C.M.D. performed research; A.T.L.L., Y.G., Y.-S.C., H.Z., C.M.D., R.W.C., X.W., Y.L., L.H.T., and E.X.W. analyzed data; and A.T.L.L., Y.G., and E.X.W. wrote the paper.

The authors declare no conflict of interest.

This article is a PNAS Direct Submission.

[1]To whom correspondence should be addressed. Email: ewu@eee.hku.hk.

This article contains supporting information online at www.pnas.org/lookup/suppl/doi:10.1073/pnas.1812453116/-/DCSupplemental.

Published online April 26, 2019.

Blood oxygen level-dependent (BOLD) functional MRI (fMRI) maps localize brain functions by measuring neuronal activities throughout the brain in response to specific sensory or cognitive tasks in basic and clinical research populations. This approach revealed the topographical organization of sensory and motor regions (20–23). However, defining vestibular (i.e., balance-related, spatial orientation-related) regions and examining their functions via traditional fMRI mapping approaches is technically difficult. In general, subjects positioned inside a scanner during fMRI experiments are unable to perform vestibular tasks, such as head and body rotation and/or translation movements. To circumvent this limitation, current fMRI investigations in humans and animals utilize caloric (24), galvanic/electrical (25–27), and auditory vestibular-evoked myogenic potential (VEMP) (28–30) stimulation of the vestibular nerve.

Such stimulation techniques have provided much needed insights into the brain-wide regions that actively participate in processing vestibular input. However, limitations to these approaches, such as the specificity and nature of the stimulation, restrict their interpretation. Caloric stimulation only activates the horizontal ampullae inside the semicircular canals without affecting the other four vestibular sense organs in the inner ear (31). This technical caveat effectively limits the conclusions. In contrast, galvanic stimulation of the vestibular nerve simultaneously activates all five vestibular sense organs (32). Activating all four major vestibular nuclei simultaneously in a synchronized manner may not consistently occur under physiological conditions. Additionally, auditory VEMP stimulations, such as cervical VEMPs and ocular VEMPs, allow more specific stimulation of the inferior and superior vestibular nerve, respectively (28, 29), but likely only constitute a pure vestibular input without encompassing the multisensory integration processes in the vestibular system. Taken together, these techniques cannot stimulate individual vestibular nuclei: the major hub of multisensory ascending and descending projections of the vestibular system. Given these technical limitations, we still have incomplete visualization of brain-wide central vestibular pathways that mediate vestibular sensory information processing.

In this study, we sought to map and categorize the downstream targets of one of the four major vestibular nuclei, the medial vestibular nucleus (MVN), across multisynaptic pathways throughout the brain via the combined use of optogenetics and fMRI (33, 34). We selectively drove expression of the optogenetic construct channelrhodopsin-2 (ChR2) in the excitatory neurons of the MVN through a Ca^{2+}/calmodulin-dependent protein kinase IIα (CaMKIIα) promoter. We then investigated the large-scale spatiotemporal distribution of downstream excitatory signal propagation from the MVN along central vestibular pathways and characterized the modulatory effects of MVN stimulation on auditory and visual processing at the cortical, thalamic, and midbrain regions.

Results

Brain-Wide fMRI Mapping of Downstream Signal Propagation from the MVN. We expressed CaMKIIα-dependent ChR2(H134R) fused with mCherry in MVN excitatory neurons in normal adult Sprague–Dawley rats (Fig. 1*A* and *SI Appendix*, Fig. S1*A*). We confirmed specific expression in MVN excitatory neurons through colocalization of mCherry with CaMKIIα staining and verification of their monosynaptic projection targets to the contralateral MVN, contralateral OMN, and ipsilateral ventral anterior (VA) and ventral posterior (VP) thalamus that matched the findings documented in experiments cataloged in the Allen Mouse Brain Connectivity Atlas (35) and from published anatomical tracing studies (1, 9, 6, 36–38) (*SI Appendix*, Fig. S1*B*). Note that CaMKIIα promoter transfects broad subtypes of MVN excitatory neurons, and hence is unable to selectively transfect any individual subtypes of MVN excitatory neurons. We performed optogenetic stimulation in lightly anesthetized adult rats (1% isoflurane). Blue-light pulses at 20 Hz (pulse width = 10 ms, light intensity = 40 mW/mm^2) were delivered to MVN neurons in a block-designed paradigm (Fig. 1*B*). This frequency matched the previously reported range of MVN neuronal firing rates (20–40 Hz) (39). The spatial spread from the fiber tip for 473-nm blue light was small (200 μm and 350 μm at 50% and 10% of initial light intensity, respectively) and had little or no spreading in the backward direction (40). Given the size of the MVN (~1 mm), optogenetic stimulation was confined within the MVN. To deliver blue-light pulses to the target region, specifically the MVN excitatory neurons, we made the exposed optical fiber cannula opaque using heat-shrinkable sleeves to prevent light leakage that may cause undesired visual stimulation.

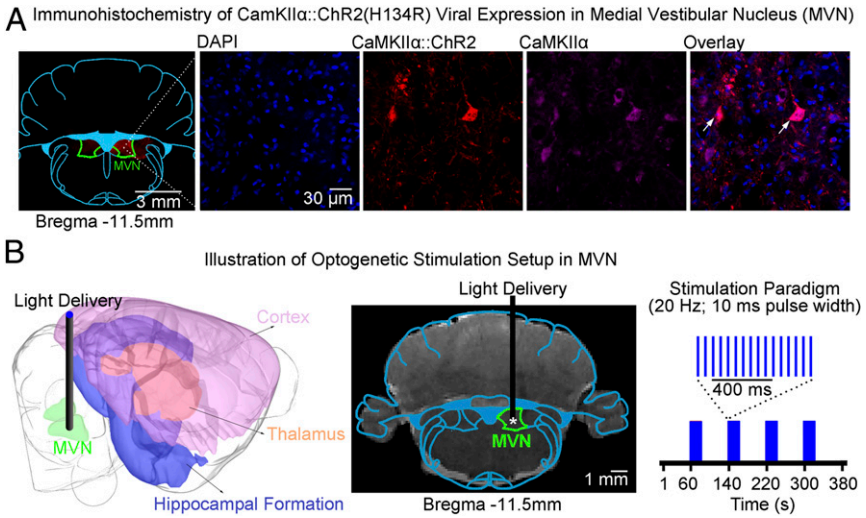

Fig. 1. Illustration of optogenetic fMRI stimulation setup and histological characterization of CaMKIIα::ChR2 viral expression in MVN excitatory neurons. (*A*) Confocal images of ChR2-mCherry expression in MVN: lower magnification (*Left*) and higher magnification (*Right*). An overlay of images costained for the nuclear marker DAPI, excitatory marker CaMKIIα, and mCherry revealed colocalization of mCherry and CaMKIIα in the cell body of MVN neurons (indicated by white arrows). (*B*, *Left*) Illustration of the stimulation site in ChR2 MVN excitatory neurons during optogenetic fMRI experiments. (*B*, *Center*) T2-weighted anatomical MRI image showing the location of the implanted optical fiber (asterisk indicates the stimulation site). (*B*, *Right*) Blue light pulses (20 Hz) with a pulse width of 10 ms were presented in a block-designed manner (20 s on and 60 s off, four blocks).

We detected robust large-scale BOLD fMRI activation bilaterally at numerous cortical, hippocampal formation, thalamic, and midbrain regions during 20-Hz ipsilateral MVN stimulation (Fig. 2 *B* and *C*). This result reveals recruitment of brain-wide and population-wide neural activity by the vestibular nucleus (VN). Notable activated regions include the sensorimotor cortices and their associated thalamus [i.e., auditory: auditory cortex (A1 & A2) and medial geniculate body (MGB); visual: visual cortex (V1 & V2), lateral posterior thalamus (LP), and lateral geniculate nucleus (LGN); motor: M1 & M2 and VA; somatosensory: somatosensory cortex (S1 & S2) and VP], high-order cortices involved in cognition [retrosplenial cortex (Rsp), cingulate cortex (Cg), temporal association cortex (TeA), and parietal cortex (Pt)], and the hippocampal formation involved in

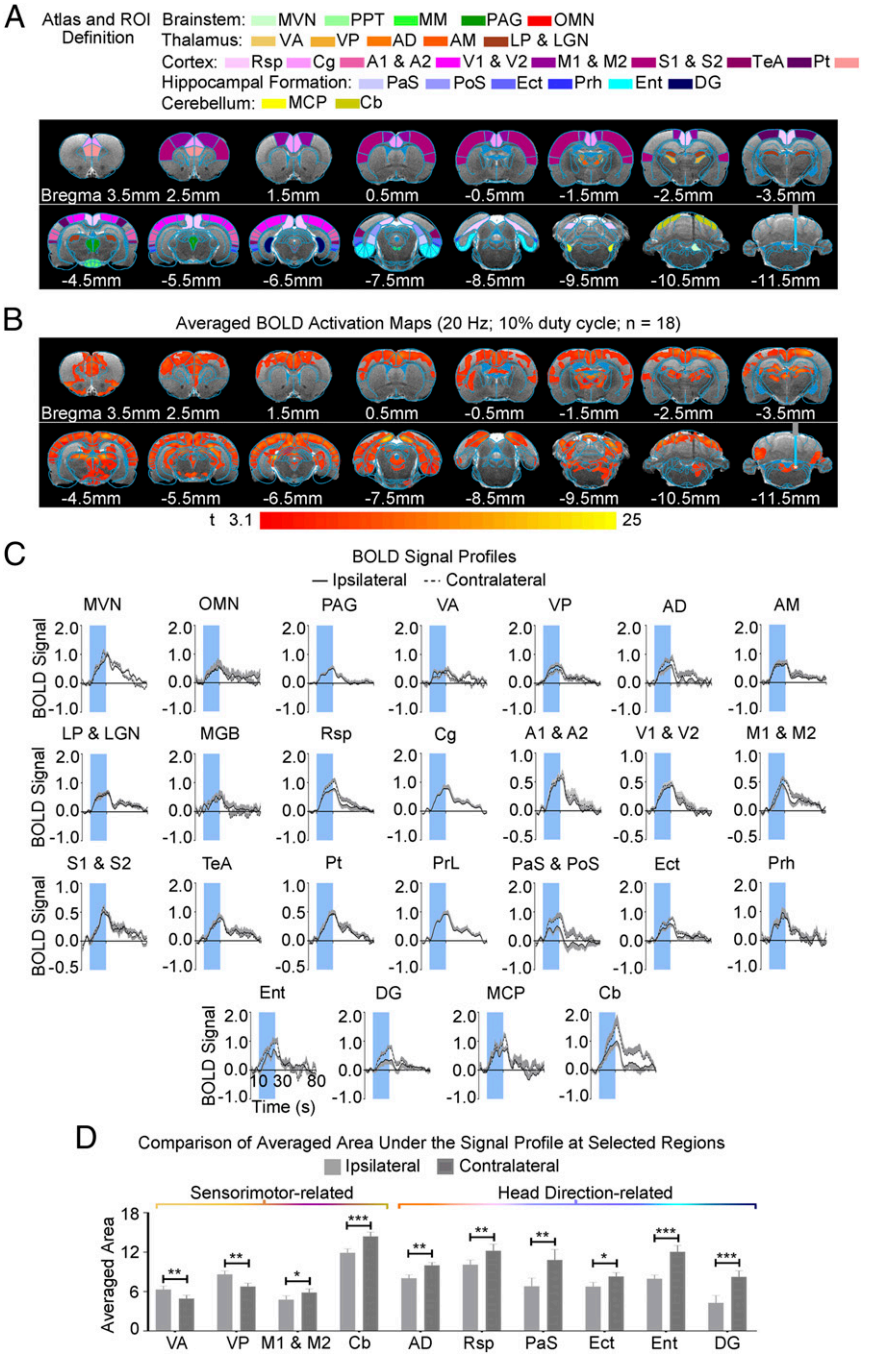

Fig. 2. Brain-wide activation at cortical and subcortical regions upon optogenetic stimulation of MVN excitatory neurons. (*A*) Illustration of Paxinos atlas-based (67) region of interest (ROI) definitions in the vestibular and midbrain (green), thalamic (orange), cortical (purple), and hippocampal formation (blue) regions. AM, anteromedial thalamus; MCP, middle cerebellar peduncle; PrL, prelimbic cortex; VL, ventrolateral thalamus. (*B*) Averaged BOLD activation maps at 20-Hz optogenetic stimulation generated by fitting a canonical HRF to individual voxels in the fMRI image ($n = 18$; $P < 0.001$; asterisk indicates the stimulation site). (*C*) BOLD signal profiles extracted from ROIs defined in *A* (error bars indicate ± SEM). (*D*) Summary of averaged area under the signal profiles at selected regions that showed significant differences in their activation strengths between hemispheres (error bars indicate ± SEM; ***$P < 0.001$, **$P < 0.01$, and *$P < 0.05$ by paired sample *t* test).

spatial navigation [subiculum: parasubiculum (PaS), postsubiculum (PoS), ectorhinal cortex (Ect), entorhinal cortex (Ent), and dentate gyrus (DG)]. Further, we found broad activation in the midbrain, which has extensive projections to thalamic and hippocampal formation regions [mammillary nucleus (MM) and periaqueductal gray (PAG)]. As expected, we also found activation of the OMN, an essential midbrain region mediating the vestibulo-ocular reflex.

We also found significant differences in the BOLD activation strength between hemispheres at key regions related to sensorimotor functions and head-direction signal processing. In regions related to sensorimotor functions, the motor and somatosensory thalami ipsilateral to the stimulated MVN, VA and VP, showed stronger activity, while the M1 & M2 and cerebellar cortex (Cb) displayed stronger contralateral activations (Fig. 2*D*; $n = 18$; VA, $P < 0.01$; VP, $P < 0.01$; M1 & M2, $P < 0.05$; Cb, $P < 0.001$ by paired sample t test). In regions associated with processing head-direction signals, such as the anterodorsal thalamus (AD), Rsp, and hippocampal formation regions (i.e., PaS, PoS, Ect, Ent, and DG), we found activations biased to the contralateral hemisphere (Fig. 2*D*; $n = 18$; AD, $P < 0.01$; Rsp, $P < 0.01$; PaS, PoS, $P < 0.01$; Ect, $P < 0.05$; Ent, $P < 0.001$; DG, $P < 0.001$ by paired sample t test).

The above fMRI visualization of large-scale vestibulo-cortical downstream signal propagation demonstrates that evoked activations are not restricted to monosynaptic efferent projections from the MVN to midbrain and thalamic regions (*SI Appendix*, Fig. S1*B*). Together, these fMRI results indicate that excitatory signals evoked by optogenetic stimulation of the MVN robustly propagate to remote cortical regions polysynaptically.

Modulatory Effects of the Vestibular System on Auditory Processing. To explore large-scale modulatory effects from the vestibular system on cortical and subcortical processing of auditory stimuli, we used a dual-stimulation paradigm with monoaural auditory stimulation and 20-Hz MVN optogenetic stimulation (Fig. 3*A*). Auditory stimulation was presented before (baseline), during optogenetic (OG; OG-On), and after (OG-Off) MVN stimulation. Note that we delivered optogenetic stimulation from 10 s before to 10 s after each sound-on period. This ensured that the BOLD response to sound was not contaminated by optogenetically evoked activations, particularly in the A1 & A2 and MGB.

Baseline monoaural auditory stimulation to the contralateral ear of animals evoked positive BOLD responses along the auditory pathway in the ipsilateral hemisphere, including the lateral lemniscus (LL), inferior colliculus (IC), MGB, and A1 & A2 (Fig. 3*B*). This finding was expected and consistent with our previous studies (21, 41). In the presence of optogenetic stimulation at the ipsilateral MVN, auditory-evoked BOLD responses significantly increased in the ipsilateral IC, MGB, and A1 & A2 (Fig. 3*C*; $n = 10$; ipsilateral IC, $P < 0.001$; ipsilateral MGB, $P < 0.05$; ipsilateral A1 & A2, $P < 0.01$ by one-way ANOVA with post hoc Bonferroni correction). However, responses in the ipsilateral LL showed a trend toward increasing during ipsilateral MVN optogenetic stimulation but were not significant. In addition, BOLD responses did not appear to remain elevated in the ipsilateral IC and MGB after cessation of optogenetic stimulation during the ~2.5-h experimental window (Fig. 3*C*). These findings demonstrate the differential modulatory effects of the vestibular system at different regions along the auditory pathway. Moreover, the results suggest that modulatory effects may be weak or absent at lower level auditory midbrain/brainstem regions (e.g., LL).

Modulatory Effects of the Vestibular System on Visual Processing. We then took the same approach and examined large-scale modulatory effects of the vestibular system on visual processing. Despite drawing methodological parallels with the combined auditory and optogenetic stimulation experiment, we presented binocular, not monocular, visual stimulation (Fig. 4*A*). This provides an

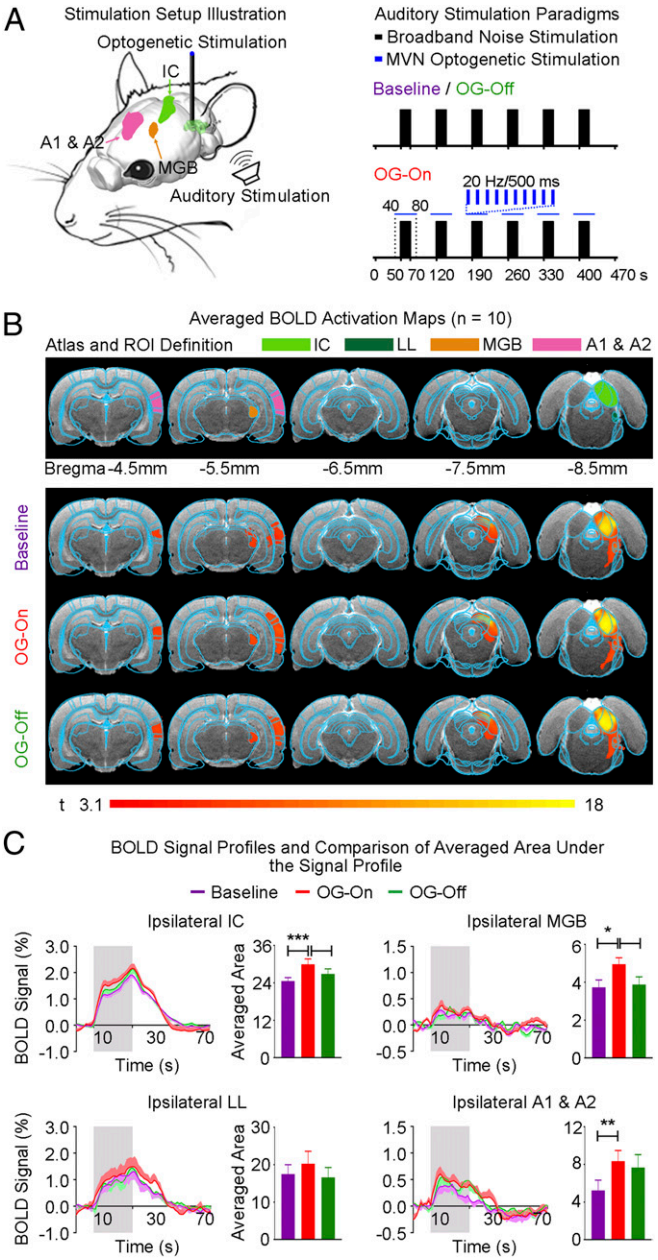

Fig. 3. MVN optogenetic stimulation enhances responses in the ipsilateral A1 & A2, thalamus (MGB), and midbrain (IC) to sound. (*A*, *Left*) Illustration of auditory and optogenetic fMRI stimulation setup. Sound was presented monoaurally to the ear contralateral to the stimulated MVN of animals. (*A*, *Right*) Broadband noise (bandwidth: 1–40 kHz; sound pressure level: 90 dB) was presented in blocks of 20 s sound-on and 50 s sound-off before (baseline), during (OG-On), and after (OG-Off) 20-Hz optogenetic stimulation. Optogenetic blue-light pulses were presented from 10 s before to 10 s after each sound-on period. Typically, five baseline auditory fMRI scans were acquired before five OG-On scans were interleaved with five OG-Off scans. (*B*, *Top*) Illustration of atlas-based region of interest (ROI) definitions. (*B*, *Bottom*) Averaged BOLD activation maps before, during, and after 20-Hz optogenetic stimulation generated by fitting a canonical HRF to individual voxels in the fMRI image ($n = 10$; $P < 0.001$). (*C*) BOLD signal profiles extracted from ROIs defined in *B* and their corresponding averaged area under the signal profile (error bars indicate ± SEM; ***$P < 0.001$, **$P < 0.01$, and *$P < 0.05$ by one-way ANOVA with post hoc Bonferroni correction). BOLD responses were enhanced in the ipsilateral A1 & A2, MGB, and IC during optogenetic stimulation. These findings indicate that the auditory pathway from the midbrain to the cortical level is modulated by central vestibular pathways.

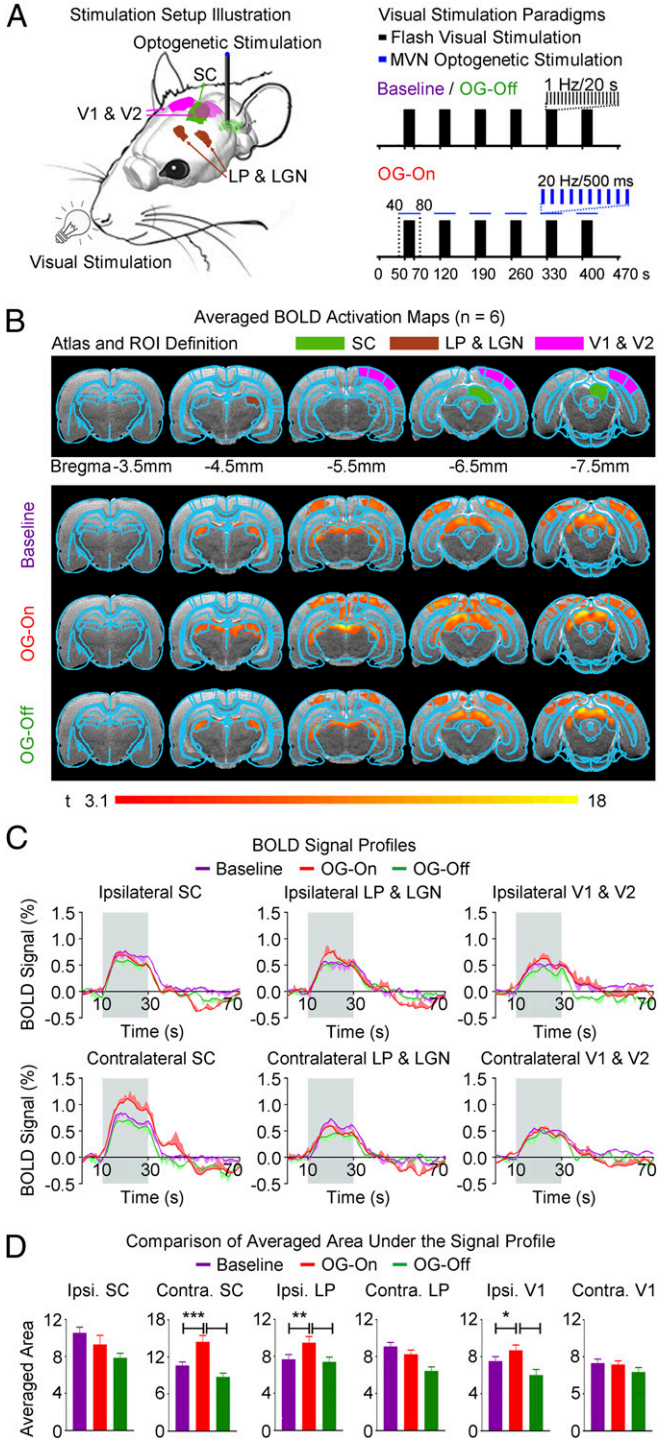

Fig. 4. MVN optogenetic stimulation enhances visually evoked responses in the ipsilateral visual cortex (V1 & V2), thalamus (LP and LGN), and contralateral subcortical SC. (*A*, *Left*) Illustration of visual and optogenetic fMRI stimulation setup. A visual stimulus was presented binocularly, while the ipsilateral MVN was optogenetically stimulated. (*A*, *Right*) Blue-light flash stimulus (frequency: 1 Hz at 10% duty cycle; intensity: 0.5 mW) was presented in blocks of 20 s flash-on and 50 s flash-off before (baseline), during (OG-On), and after (OG-Off) 20-Hz optogenetic stimulation. Optogenetic blue-light pulses were presented from 10 s before to 10 s after each flash-on period. Typically, five baseline visual fMRI scans were acquired before five OG-On scans were interleaved with five OG-Off scans. (*B*, *Top*) Illustration of atlas-based region of interest (ROI) definitions. (*B*, *Bottom*) Averaged BOLD activation maps before, during, and after 20-Hz optogenetic stimulation generated by fitting a canonical HRF to individual voxels in the fMRI image ($n = 6$; $P < 0.001$). (*C* and *D*) BOLD signal profiles extracted from ROIs defined in *B* and their corresponding averaged area under the signal profile (error bars indicate ± SEM; $***P < 0.001$, $**P < 0.01$, and $*P < 0.05$ by one-way ANOVA with post hoc Bonferroni correction). Optogenetic stimulation enhanced BOLD responses in the ipsilateral (Ipsi.) V1 & V2 and LGN, but not their contralateral (Contra.) counterparts. The opposite, however, was true for responses in the SC, which showed enhanced responses in the contralateral, not ipsilateral, SC. These findings indicate that the visual pathway is differentially modulated at thalamic and cortical regions and at the midbrain SC by central vestibular pathways.

opportunity to examine the differences in modulatory effects between hemispheres, in addition to differences at regions along the visual pathway.

Baseline visual stimulation evoked positive BOLD responses bilaterally along the visual pathway, including the LP and LGN, superior colliculus (SC), and V1 & V2 (Fig. 4*B*). This finding was expected and consistent with the previous studies (22, 42, 43). In the presence of optogenetic stimulation at the ipsilateral MVN, visually evoked BOLD responses significantly increased in the ipsilateral LP, LGN, and V1 & V2 (Fig. 4*C*; $n = 6$; ipsilateral LP and LGN, $P < 0.01$; ipsilateral V1 & V2, $P < 0.05$ by one-way ANOVA with post hoc Bonferroni correction). Responses in the contralateral LP and LGN and V1 & V2 showed a trend of decrease during ipsilateral MVN optogenetic stimulation but were not significant. Surprisingly, we found an enhanced response in the contralateral SC rather than an increase in the ipsilateral visual midbrain SC (Fig. 4*C*; $n = 6$; contralateral SC, $P < 0.001$ by one-way ANOVA with post hoc Bonferroni correction). This finding parallels our observations in the auditory midbrain IC. BOLD responses also did not remain elevated in the ipsilateral LP and LGN, ipsilateral V1 & V2, and contralateral SC after cessation of optogenetic stimulation during the ∼2.5-h experimental window (Fig. 4*C*). These findings demonstrate an added dimension to the numerous factors that determine the differential modulatory effects of the vestibular system on sensory processing. In summary, we demonstrate that modulatory effects have hemispheric differences and are under the influence of the different functional roles played by individual regions along their respective sensory pathways (e.g., SC vs. IC).

Note that in all optogenetic fMRI experiments, we did not use the β values [i.e., as generated via a general linear model by fitting a canonical hemodynamic response function (HRF) to each voxel in the fMRI image] to quantify the activation strength for comparison across different regions (Fig. 2*D*) and different experimental conditions (Figs. 3*D* and 4*D*). The reason was that the BOLD signal temporal profiles extracted (Figs. 2*B*, 3*C*, and 4*C*) showed some deviations from the canonical HRF, making the quantitation prone to errors and unsuitable for comparisons. Instead, we computed the area under the signal profile (more details are provided in *SI Appendix, SI Methods*).

Discussion

The vestibular system differs vastly from other primary sensory systems, such as the auditory, visual, and somatosensory systems. These other systems are organized in a topographic and orderly fashion, whereby projections from peripheral sense organs course through a modality-specific primary thalamic nucleus before reaching their primary cortical targets (e.g., MGB to auditory cortex, AC, in the auditory system) (44). However, the vestibular system encompasses a more complex organization of its pathways with overlapping inputs from sense organs and other sensory thalamic nuclei to individual vestibular nuclei and numerous efferent projections from the vestibular nuclei across hemispheres to sensory/nonsensory midbrain regions and the hippocampal formation (1, 45). Moreover, unlike primary sensory processing, central vestibular processing is distributed across multiple regions (46). Given these complexities and challenges,

studies to examine the broad range of neural targets of individual vestibular nuclei and explore the modulatory effects of the vestibular system on sensory processing remain scarce.

Here, we monitored large-scale neural responses during MVN optogenetic stimulation using brain-wide fMRI. Our fMRI results showed robust bilateral activations at numerous regions, such as sensorimotor cortices and their associated thalamic nuclei (i.e., auditory, visual, motor, somatosensory), higher order cortices involved in cognition (i.e., Rsp, Cg, TeA, Pt), and hippocampal regions involved in spatial navigation (i.e., subiculum, Ent, DG). During ipsilateral MVN stimulation, we also found significantly enhanced responses to auditory or visual stimulation in auditory and visual cortical and thalamic regions ipsilateral to the stimulated MVN (A1 & A2 and MGB, and V1 & V2, LP and LGN, respectively). We also found elevated responses in the auditory and visual midbrain, ipsilateral IC, and contralateral SC. These findings indicate differential effects of optogenetic stimulation on sensory-evoked responses along the auditory and visual sensory pathways. Together, these results successfully demonstrate the capability of using fMRI to map brain-wide central vestibular pathways and reveal large-scale modulatory effects of the vestibular system on sensory processing.

Mapping of Central Vestibular Pathways and the Question of Hemispheric Dominance. Despite the wealth of evidence describing the anatomical projections within the vestibular system (6, 7, 9, 47–49) and key investigations through functional imaging (i.e., fMRI, positron emission tomography) (25–27, 50, 51), key questions remain. What is the spatial extent of vestibular processing in the brain? This question remains due to the unique technical challenges presented by stimulating the vestibular system and ensuring no movement artifacts (stationary and stable) during functional imaging, as well as the inability to stimulate each individual VN separately. One can argue that current advances in dense electrophysiological recordings would be advantageous in circumventing the need for subjects to remain still because recordings can be performed in freely moving subjects. However, it remains an unrealistic experimental proposition to place tens of recording electrodes that span the entire brain, particularly those that use invasive recordings in deep brain regions, such as the brainstem, thalamus, and hippocampus.

To achieve a more holistic visualization of the brain-wide central vestibular pathways, we deployed a strategy to circumvent the two aforementioned challenges. Instead of stimulating the vestibular labyrinth or nerve, we optogenetically stimulated the MVN. This approach yielded specificity to initiate activity from one of the four well-defined vestibular nuclei, ensure the animal remains stationary, and use large-view fMRI. We found activations at numerous subcortical and cortical regions not shown in previous functional imaging studies (16, 26, 27, 51), such as the MM, PAG, AD, and DG, as well as the PaS, PoS, Ect, Ent, V1 & V2, A1 & A2, M1 & M2, prelimbic cortex, and Cb. This finding demonstrates the strength of our approach in revealing the spatial extent of vestibular processing in the brain, specifically engaging the hippocampal formation and cortex, while corroborating direct projections between the MVN and thalamus or midbrain regions (1, 9, 37). We also observed more robust activations in posterior brain regions, specifically the DG, and in comparisons between sensory cortices (i.e., V1 & V2 and A1 & A2 vs. S1 & S2). This observation suggests a functional axis in central vestibular pathway organization for each VN.

What is the distribution of vestibular processing between and across the two hemispheres? Quantifying the activation strength of the BOLD signal profiles (Fig. 2 *C* and *D*) showed hemispheric differences in specific midbrain, thalamic, hippocampal formation, and cerebellar regions. The VA and VP showed significant ipsilateral dominance. Such observations corroborate our histological slices demonstrating direct ipsilateral projections to VA and VP (*SI Appendix*, Fig. S1*B*). Using similar adeno-associated virus (AAV)-mediated monosynaptic tracing methods, the Allen mouse brain connectivity atlas database also described these projections to the VA and VP (experiment ID 480689656) (35). However, the ipsilateral dominance in the VA and VP did not extend to the M1 & M2 and S1 & S2, suggesting that these two cortical regions do not linearly represent the responses from their associated thalamic nuclei (52). Interestingly, we found contralateral hemispheric dominance in activated hippocampal, thalamic, and high-order cortical regions, such as the PaS, PoS, Ect, Ent, DG, AD, and Rsp. Studies propose that these regions comprise the head direction pathway (3, 5). However, our histological slices showed predominant projections to the ipsilateral, not contralateral, AD (*SI Appendix*, Fig. S1*B*). We were unable to visualize the projections from the MVN to the hippocampal formation and cortical regions due to the limits of monosynaptic labeling using the AAV tracers (40). We also found contralateral dominance in the Cb and M1 & M2, indicating interactions and/or hemispheric lateralization of functions that may underlie compensatory motor actions during vestibular processing (4).

Based on our fMRI findings, we categorized four distinct central vestibular pathways from the MVN (Fig. 5), namely, the

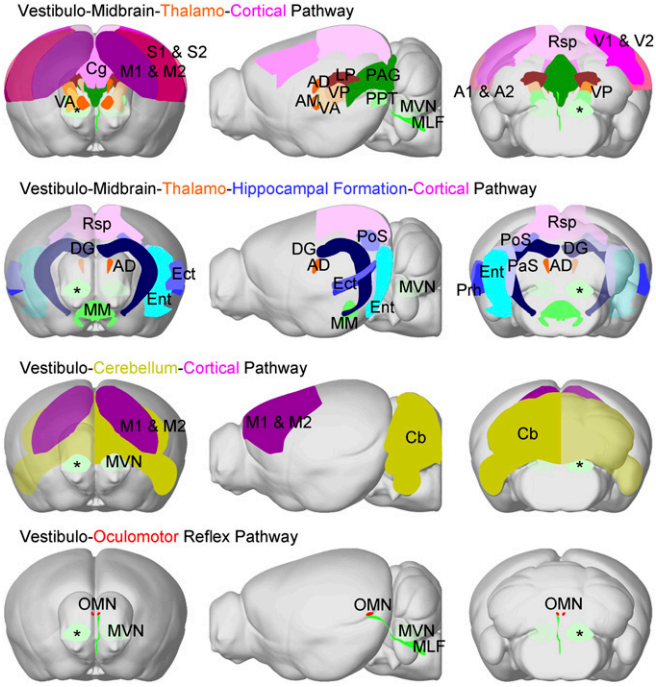

Fig. 5. Categorization of distinct brain-wide central vestibular pathways activated by optogenetic stimulation of MVN excitatory neurons. We categorized four distinct pathways based on the activated regions detected by BOLD fMRI in Fig. 2. Note that the color used to define each region is scaled to the mean activation strength as quantified by the averaged area under the BOLD signal profile in Fig. 2C. The vestibulo-midbrain-thalamo-cortical pathway and ipsilateral VA and VP showed stronger activations than their contralateral counterparts. This indicates that monosynaptic projections from the site of stimulation in the ipsilateral MVN (*) directly drove activation in the motor and somatosensory thalamus. In the vestibulo-midbrain-thalamo-hippocampal formation cortical and vestibulo-midbrain-hippocampal formation pathways, the majority of hippocampal formation regions (PaS, PoS, Ect, Ent, and DG), a cortical region (Rsp), and a thalamic region (AD) displayed stronger contralateral activations. These regions participate in processing head direction signals (3, 5). The vestibulo-cerebellum-cortical pathway displayed stronger activations at the contralateral Cb and M1 & M2, indicating key interactions underlying vestibulo-motor functions. In the vestibulo-oculomotor reflex pathway, both activated OMNs did not show hemispheric differences despite only receiving direct projections contralaterally from the MVN. AM, anteromedial thalamus.

(*i*) vestibulo-midbrain-thalamo-cortical pathway, (*ii*) vestibulo-midbrain-thalamo-hippocampal formation and vestibulo-midbrain-hippocampal formation pathway, (*iii*) vestibulo-cerebellar pathway, and (*iv*) vestibulo-oculomotor reflex pathway. Critically, we presented direct evidence of activations in the AD and across numerous hippocampal formation regions (i.e., PaS, PoS, Ect, Ent, DG). This finding indicates that these regions actively participate in processing head direction signals and spatial perception, which were only suggested previously (3, 5, 53, 54), given their respective roles in spatial memory and navigation. Our fMRI findings also corroborated the previously published description of projection targets from the MVN to the cerebellum (1), sensory and motor thalamus (37), OMN in the midbrain (13), and contralateral MVN (49). Taken together, our fMRI observations of hemispheric dominance suggest functional differences in these different central vestibular pathways (39, 55). These findings will be crucial for future investigations of central vestibular processing.

Differential Modulatory Effects of the Vestibular System on Auditory and Visual Processing. The vestibular system integrates input from our other dominant senses, such as audition, vision, and sensation, to create a multisensory percept with respect to our body's reference frame. Such integration is vital for accurate processing of bodily senses (17, 56). For example, the vestibulo-oculomotor pathway, which senses head rotational motion, produces an involuntary reflex in our eyes to ensure our perception of the visual field remains stationary. However, we do not know the extent of modulatory effects (if any) that the vestibular system exerts on sensory processing. In our study, we specifically addressed this in relation to auditory and visual processing at cortical, thalamic, and midbrain regions.

We found that activation of central vestibular pathways from the ipsilateral MVN enhanced both ipsilateral cortex and auditory and visual thalamic pathways (i.e., A1 & A2 and MGB, and V1 & V2, LP and LGN, respectively). However, we did not observe such enhancement in the contralateral V1 & V2 and thalamus, indicating differences in hemispheric modulatory effects by the vestibular system on sensory processing. Proposed multisensory processing mechanisms rely on hemispheric dominance or lateralization of vestibular functions (38, 55, 57–59). In particular, the activity dominance shown in our study shifted to the hemisphere ipsilateral to the stimulated vestibular labyrinth and VN. So, our observation of the enhancement at ipsilateral, not contralateral, cortical and thalamic regions suggests activating the vestibular system dynamically shifts the excitability of the auditory and visual pathways to bias the hemisphere ipsilateral to the MVN stimulation. When comparing the auditory and visual midbrain, we surprisingly discovered different hemispheric activations that showed enhanced ipsilateral IC and contralateral SC. This key observation indicates an additional factor that can influence the extent of modulatory effects across both hemispheres. Specifically, our findings suggest different functional roles that the SC and IC play in their respective sensory processing pathways. The SC can mediate visual saccades (60), which occur during the optokinetic nystagmus. So, the effect we observed in the contralateral, not ipsilateral, SC could reflect the strong bias exerted by the vestibulo-oculomotor pathway that predominantly projects to and activates the contralateral hemisphere, as shown in our finding (*SI Appendix*, Fig. S1*B*) and by others (1, 61).

Physiological Effects of a Strong Magnetic Field During MRI on the Vestibular System. Transient dizziness and vertigo in humans in the presence of a strong magnetic field, such as in the MRI scanner, have been reported as early as the 1990s (62). Experiments have been conducted to measure the psychophysiological correlates of the reported discomforts experienced by subjects in the high-field MRI scanners (63). While the outcomes of these measures strongly indicate the psychophysiological effects at a high magnetic field (e.g., 7 T), the sensations of transient dizziness and vertigo perceived by subjects have been inconsistent among studies and even subjects within the same study. However, these studies consistently reported robust nystagmus when subjects lay down inside the MRI scanner. It was proposed that magnetohydrodynamics forces, particularly the Lorentzian forces from the interactions between the magnetic field and ionic currents in the labyrinth, were pushing against the semicircular canal cupula and causing nystagmus (64).

It is worth noting that the bulk of literature on the effects of a static magnetic field on the vestibular system discussed above were studies of humans, but not animals. Although there are studies performed on rodents that showed physiological effects of high-field MRI scanners on the animal behavior (65, 66), there is a limited understanding of the large-scale effects of magnetic fields on the vestibular system. Indeed, these physiological effects can be complex, and more in-depth investigations to localize and identify the effects of a static magnetic field on the central nervous system during fMRI are desired in the future.

In summary, our results directly reveal brain-wide central vestibular pathways from the MVN that span multiple hierarchical levels, ranging from the brainstem to the thalamus, hippocampal formation, and cortex. In addition, we show the extent of large-scale modulatory effects of the vestibular system on visual and auditory processing. As such, this study presents the combined use of large-view fMRI, optogenetic neuromodulation, and external stimuli as a valuable means to dissect complex brain systems and their functions over a large scale. Our findings here will spur future in-depth investigations into the key mechanisms underlying activations of distinct central vestibular pathways and vestibular multisensory processing.

Methods

Animal Subjects. Adult male Sprague–Dawley rats were used in all experiments. Animals were individually housed under a 12-h light/dark cycle with access to food and water ad libitum. All animal experiments were approved by Committee on the Use of Live Animals in Teaching and Research of the University of Hong Kong. Three groups of animals were used: group I (n = 18) for optogenetic fMRI experiments, group II (n = 10) for combined auditory and optogenetic stimulation, and group III (n = 6) for combined visual and optogenetic fMRI experiments. Full details of animal surgical procedures, optogenetic stimulation paradigms, fMRI acquisition and analysis procedures, and histology are provided in *SI Appendix*, *SI Methods*.

Data and Code Availability. The data that support the findings of this study and computer codes used are available from the corresponding author upon request.

ACKNOWLEDGMENTS. We thank Drs. A. To, M. Lyu, and H. Lei, and Ms. M. C. Yang for their technical assistance. We also thank Dr. K. Deisseroth, who provided us with the ChR2 viral construct. This work was supported by the Hong Kong Research Grant Council (Grants C7048-16G and HKU17103015 to E.X.W.), Lam Woo Foundation, Shenzhen Municipal Brain Science Platform Technology Project, and 2018–2019 Guangdong Provincial Key Brain Science and Research Project.

1. Vidal PP, et al. (2015) The vestibular system. *The Rat Nervous System*, ed Paxinos G (Academic, San Diego), pp 805–864.
2. Goldberg JM (2013) Vestibular inputs: The vestibular system. *Neuroscience in the 21st Century*, ed Pfaff DW (Springer New York, New York), pp 883–929.
3. Hitier M, Besnard S, Smith PF (2014) Vestibular pathways involved in cognition. *Front Integr Neurosci* 8:59.
4. Cullen KE (2012) The vestibular system: Multimodal integration and encoding of self-motion for motor control. *Trends Neurosci* 35:185–196.

5. Cullen KE, Taube JS (2017) Our sense of direction: Progress, controversies and challenges. *Nat Neurosci* 20:1465–1473.
6. Shiroyama T, Kayahara T, Yasui Y, Nomura J, Nakano K (1999) Projections of the vestibular nuclei to the thalamus in the rat: A Phaseolus vulgaris leucoagglutinin study. *J Comp Neurol* 407:318–332.
7. Lai H, et al. (2000) Morphological evidence for a vestibulo-thalamo-striatal pathway via the parafascicular nucleus in the rat. *Brain Res* 872:208–214.
8. Teune TM, van der Burg J, van der Moer J, Voogd J, Ruigrok TJ (2000) Topography of cerebellar nuclear projections to the brain stem in the rat. *Prog Brain Res* 124: 141–172.
9. Kotchabhakdi N, Rinvik E, Walberg F, Yingchareon K (1980) The vestibulothalamic projections in the cat studied by retrograde axonal transport of horseradish peroxidase. *Exp Brain Res* 40:405–418.
10. Meng H, May PJ, Dickman JD, Angelaki DE (2007) Vestibular signals in primate thalamus: Properties and origins. *J Neurosci* 27:13590–13602.
11. Waespe W, Henn V (1977) Neuronal activity in the vestibular nuclei of the alert monkey during vestibular and optokinetic stimulation. *Exp Brain Res* 27:523–538.
12. Waespe W, Henn V (1979) The velocity response of vestibular nucleus neurons during vestibular, visual, and combined angular acceleration. *Exp Brain Res* 37:337–347.
13. Blackwood W, Dix MR, Rudge P (1975) The cerebral pathways of optokinetic nystagmus: A neuro-anatomical study. *Brain* 98:297–308.
14. Precht W, Strata P (1980) On the pathway mediating optokinetic responses in vestibular nuclear neurons. *Neuroscience* 5:777–787.
15. Dieterich M, Bucher SF, Seelos KC, Brandt T (1998) Horizontal or vertical optokinetic stimulation activates visual motion-sensitive, ocular motor and vestibular cortex areas with right hemispheric dominance. An fMRI study. *Brain* 121:1479–1495.
16. Kirsch V, et al. (2016) Structural and functional connectivity mapping of the vestibular circuitry from human brainstem to cortex. *Brain Struct Funct* 221:1291–1308.
17. Angelaki DE, Cullen KE (2008) Vestibular system: The many facets of a multimodal sense. *Annu Rev Neurosci* 31:125–150.
18. Smith PF, et al. (2005) The effects of vestibular lesions on hippocampal function in rats. *Prog Neurobiol* 75:391–405.
19. Brandt T, et al. (2005) Vestibular loss causes hippocampal atrophy and impaired spatial memory in humans. *Brain* 128:2732–2741.
20. Belliveau JW, et al. (1991) Functional mapping of the human visual cortex by magnetic resonance imaging. *Science* 254:716–719.
21. Cheung MM, et al. (2012) BOLD fMRI investigation of the rat auditory pathway and tonotopic organization. *Neuroimage* 60:1205–1211.
22. Pawela CP, et al. (2008) Modeling of region-specific fMRI BOLD neurovascular response functions in rat brain reveals residual differences that correlate with the differences in regional evoked potentials. *Neuroimage* 41:525–534.
23. Silva AC, Koretsky AP (2002) Laminar specificity of functional MRI onset times during somatosensory stimulation in rat. *Proc Natl Acad Sci USA* 99:15182–15187.
24. Suzuki M, et al. (2001) Cortical and subcortical vestibular response to caloric stimulation detected by functional magnetic resonance imaging. *Brain Res Cogn Brain Res* 12:441–449.
25. Lobel E, Kleine JF, Bihan DL, Leroy-Willig A, Berthoz A (1998) Functional MRI of galvanic vestibular stimulation. *J Neurophysiol* 80:2699–2709.
26. Dieterich M, Brandt T (2008) Functional brain imaging of peripheral and central vestibular disorders. *Brain* 131:2538–2552.
27. Rancz EA, et al. (2015) Widespread vestibular activation of the rodent cortex. *J Neurosci* 35:5926–5934.
28. de Waele C (2001) VEMP induced by high level clicks. A new test of saccular otolith function. *Adv Otorhinolaryngol* 58:98–109.
29. Colebatch JG, Halmagyi GM, Skuse NF (1994) Myogenic potentials generated by a click-evoked vestibulocollic reflex. *J Neurol Neurosurg Psychiatry* 57:190–197.
30. Schlindwein P, et al. (2008) Cortical representation of saccular vestibular stimulation: VEMPs in fMRI. *Neuroimage* 39:19–31.
31. Furman JM, Wuyts FL (2012) Vestibular laboratory testing. *Aminoff's Electrodiagnosis in Clinical Neurology* (Saunders, London), pp 699–723.
32. Palla A, Lenggenhager B (2014) Ways to investigate vestibular contributions to cognitive processes. *Front Integr Neurosci* 8:40.
33. Lee JH, et al. (2010) Global and local fMRI signals driven by neurons defined optogenetically by type and wiring. *Nature* 465:788–792.
34. Leong AT, et al. (2016) Long-range projections coordinate distributed brain-wide neural activity with a specific spatiotemporal profile. *Proc Natl Acad Sci USA* 113: E8306–E8315.
35. Oh SW, et al. (2014) A mesoscale connectome of the mouse brain. *Nature* 508: 207–214.
36. Zwergal A, Strupp M, Brandt T, Büttner-Ennever JA (2009) Parallel ascending vestibular pathways: Anatomical localization and functional specialization. *Ann N Y Acad Sci* 1164:51–59.
37. Lopez C, Blanke O (2011) The thalamocortical vestibular system in animals and humans. *Brain Res Brain Res Rev* 67:119–146.
38. Dieterich M, Brandt T (2015) The bilateral central vestibular system: Its pathways, functions, and disorders. *Ann N Y Acad Sci* 1343:10–26.
39. Beraneck M, Cullen KE (2007) Activity of vestibular nuclei neurons during vestibular and optokinetic stimulation in the alert mouse. *J Neurophysiol* 98:1549–1565.
40. Yizhar O, Fenno LE, Davidson TJ, Mogri M, Deisseroth K (2011) Optogenetics in neural systems. *Neuron* 71:9–34.
41. Zhang JW, et al. (2013) Functional magnetic resonance imaging of sound pressure level encoding in the rat central auditory system. *Neuroimage* 65:119–126.
42. Zhou IY, Cheung MM, Lau C, Chan KC, Wu EX (2012) Balanced steady-state free precession fMRI with intravascular susceptibility contrast agent. *Magn Reson Med* 68: 65–73.
43. Lau C, et al. (2011) BOLD responses in the superior colliculus and lateral geniculate nucleus of the rat viewing an apparent motion stimulus. *Neuroimage* 58:878–884.
44. Jones EG (2007) *The Thalamus* (Cambridge Univ Press, Cambridge, UK), 2nd Ed.
45. Lim R, Brichta AM (2012) Vestibular system. *The Mouse Nervous System*, eds Paxinos G, Puelles L (Academic, San Diego), pp 661–681.
46. Fattal D, Hansen M, Fritzsch B (2018) Aging-related balance impairment and hearing loss. *The Wiley Handbook on the Aging Mind and Brain* (Wiley, New York), pp 315–336.
47. Barmack NH (2003) Central vestibular system: Vestibular nuclei and posterior cerebellum. *Brain Res Bull* 60:511–541.
48. Brown JE, Card JP, Yates BJ (2005) Polysynaptic pathways from the vestibular nuclei to the lateral mammillary nucleus of the rat: Substrates for vestibular input to head direction cells. *Exp Brain Res* 161:47–61.
49. Highstein SM, Holstein GR (2006) *The Anatomy of the Vestibular Nuclei*, Progress in Brain Research, ed Büttner-Ennever JA, (Elsevier, Amsterdam), Vol 151, pp 157–203.
50. Lobel E, et al. (1999) Cortical areas activated by bilateral galvanic vestibular stimulation. *Ann N Y Acad Sci* 871:313–323.
51. Bense S, Stephan T, Yousry TA, Brandt T, Dieterich M (2001) Multisensory cortical signal increases and decreases during vestibular galvanic stimulation (fMRI). *J Neurophysiol* 85:886–899.
52. Laurens J, et al. (2017) Transformation of spatiotemporal dynamics in the macaque vestibular system from otolith afferents to cortex. *eLife* 6:e20787.
53. Jacob PY, Poucet B, Liberge M, Save E, Sargolini F (2014) Vestibular control of entorhinal cortex activity in spatial navigation. *Front Integr Neurosci* 8:38.
54. Smith PF, Zheng Y (2013) From ear to uncertainty: Vestibular contributions to cognitive function. *Front Integr Neurosci* 7:84.
55. Dieterich M, Brandt T (2018) Global orientation in space and the lateralization of brain functions. *Curr Opin Neurol* 31:96–104.
56. Ferrè ER, Walther LE, Haggard P (2015) Multisensory interactions between vestibular, visual and somatosensory signals. *PLoS One* 10:e0124573.
57. Oh SY, Boegle R, Ertl M, Stephan T, Dieterich M (2018) Multisensory vestibular, vestibular-auditory, and auditory network effects revealed by parametric sound pressure stimulation. *Neuroimage* 176:354–363.
58. Ueberfuhr MA, Braun A, Wiegrebe L, Grothe B, Drexl M (2017) Modulation of auditory percepts by transcutaneous electrical stimulation. *Hear Res* 350:235–243.
59. Della-Justina HM, et al. (2015) Interaction of brain areas of visual and vestibular simultaneous activity with fMRI. *Exp Brain Res* 233:237–252.
60. Lee C, Rohrer WH, Sparks DL (1988) Population coding of saccadic eye movements by neurons in the superior colliculus. *Nature* 332:357–360.
61. Dieterich M, Brandt T (1995) Vestibulo-ocular reflex. *Curr Opin Neurol* 8:83–88.
62. Kangarlu A, et al. (1999) Cognitive, cardiac, and physiological safety studies in ultra high field magnetic resonance imaging. *Magn Reson Imaging* 17:1407–1416.
63. Mian OS, Glover PM, Day BL (2015) Reconciling magnetically induced vertigo and nystagmus. *Front Neurol* 6:201.
64. Roberts DC, et al. (2011) MRI magnetic field stimulates rotational sensors of the brain. *Curr Biol* 21:1635–1640.
65. Houpt TA, Kwon B, Houpt CE, Neth B, Smith JC (2013) Orientation within a high magnetic field determines swimming direction and laterality of c-Fos induction in mice. *Am J Physiol Regul Integr Comp Physiol* 305:R793–R803.
66. Houpt TA, Pittman DW, Barranco JM, Brooks EH, Smith JC (2003) Behavioral effects of high-strength static magnetic fields on rats. *J Neurosci* 23:1498–1505.
67. Paxinos G (2007) *The Rat Brain in Stereotaxic Coordinates* (Elsevier, Amsterdam), 6th Ed.